Lab on a Chip

Characterization of syringe-pump-driven induced pressure fluctuations in elastic microchannels

Journal:	*Lab on a Chip*
Manuscript ID:	LC-ART-11-2014-001347.R2
Article Type:	Paper
Date Submitted by the Author:	16-Dec-2014
Complete List of Authors:	Zeng, Wen; Harbin Institute of Technology, Department of Fluid Control and Automation; Princeton, Mechanical and Aerospace Engineering Jacobi, Ian; Princeton University, Mechanical and Aerospace Engineering Beck, David; Princeton, Mechanical and Aerospace Engineering Li, Songjing; Harbin Institute of Technology, Department of Fluid Control and Automation Stone, Howard; Princeton, Mechanical and Aerospace Engineering

Characterization of syringe-pump-driven induced pressure fluctuations in elastic microchannels

Wen Zeng[a,b], Ian Jacobi[a], David J. Beck[a], Songjing Li*[b] and Howard A. Stone*[a]

Received Xth XXXXXXXXXX 20XX, Accepted Xth XXXXXXXXX 20XX
First published on the web Xth XXXXXXXXXX 200X
DOI: 10.1039/b000000x

We study pressure and flow-rate fluctuations in microchannels, where the flow rate is supplied by a syringe pump. We demonstrate that the pressure fluctuations are induced by the flow-rate fluctuations coming from mechanical oscillations of the pump motor. Also, we provide a mathematical model of the effect of the frequency of the pump on the normalized amplitude of pressure fluctuations and introduce a dimensionless parameter incorporating pump frequency, channel geometry and mechanical properties that can be used to predict the performance of different microfluidic device configurations. The normalized amplitude of pressure fluctuations decreases as the frequency of the pump increases and the elasticity of the channel material decreases. The mathematical model is verified experimentally over a range of typical operating conditions and possible applications are discussed.

1 Introduction

All flow systems can experience fluctuations, even when apparently steady operating conditions are imposed. In particular, the wide applicability of microfluidic systems for fluid delivery operations in chemical, materials, biological and medical processes [1–5] raises the question of characterizing the magnitudes of the pressure or flow-rate fluctuations. To the best of our knowledge, there have been few studies of these inevitable fluctuations. For example, recently Li et al.[6] provided visual evidence of the flow-rate fluctuations that arise in flow-rate driven microfluidic flows and correlated the fluctuations with the mechanical oscillations that occur with syringe pumps. Here, we document direct measurements of the pressure fluctuations in flow-rate driven microfluidic flows, and provide a mathematical model in good agreement with the data that shows lower relative pressure fluctuations for higher frequencies and in softer systems.

The mechanical response of microfluidic devices can be characterized by measuring the deformed shape of the soft channels and the pressure in the channels. For example, direct measurement of the shape of channels for pressure-driven flow have been reported.[7,8] Also, by measuring the pressure drop, the flow rate of a microchannel can be calculated and the dynamic characteristics of the microfluidic device can be determined.[9,10] Similar ideas have been demonstrated to offer a strategy for flow control in microchannels: by measuring the input and output amplitudes of the pressure in microfluidic circuits with passive elastomeric features, the effect of the frequency of a time-modulated pressure source on fluid flow can established and controlled[11].

While pressure fluctuations are often thought of as caused by flow-rate fluctuations,[12,13], pressure fluctuations can occur independently of flow-rate fluctuations, due to the deformability of elastic tubes common to many flow devices.[14] For example, such pressure fluctuations have been studied in models of physiological flows when the Reynolds number is high, e.g.[15,16] In microfluidic systems, for which the Reynolds number is typically low to moderate, e.g. $Re < 10$, syringe pumps have been used widely to supply continuous flow rates. However, although syringe pumps are a common source of flow-rate fluctuations[6], to the best of our knowledge, the magnitude of the correspond pressure and flow-rate fluctuations, and how they vary with pump frequency, geometrical features and physical properties, have not been quantified; some qualitative comments can be found in the literature, such as the remark that fluctuations in flow rate are larger at lower flow rates.[9]

In this paper, we present experimental measurements of the frequency and amplitude of syringe-pump-driven pressure fluctuations in PDMS microchannels. A model is established to explain the temporal development of pressure fluctuations as a function of pump frequency, geometrical parameters and fluid properties. Using a non-dimensional Strouhal number that compares the forcing frequency to a viscoelastic frequency, the normalized amplitude of the pressure fluctuations can be quantified. The model then suggests several methods for reducing relative pressure fluctuations in soft microchannels.

[a] *Department of Mechanical & Aerospace Engineering, Princeton University, Princeton, NJ 08544, USA. E-mail: hastone@princeton.edu*
[b] *Department of Fluid Control and Automation, Harbin Institute of Technology, Harbin, 150001, China. E-mail: lisongjing@hit.edu.cn*

2 Experimental setup

We report two types of flow-rate-driven experiments: studies of (i) pressure fluctuations and (ii) droplet generation. In particular, the droplet generation experiments will be used as a tool for characterization of the fluctuations in the flow rate. We design a T-junction microchannel to conduct these experiments. The width, height and length of the rectangular microchannels are, respectively, 100 μm × 10 μm × 100 mm. In our experiments, one type of syringe pump (Harvard Apparatus Standard Infuse/Withdraw PHD Ultra Syringe Pump) is tested. HSW syringes are used for the experiment, and the diameters D of the syringes are 4.69, 9.60, 12.45 and 15.90 mm. Water is chosen as the working liquid and the pressure drop across the system is measured. The simplified model of the experimental system is shown in Fig. 1. Here, Q_i (possibly time-varying) is the inlet flow rate and Q_o is the outlet flow rate.

The gauge pressure at the inlet of the PDMS microchannel is measured by a pressure sensor (OMEGA PX26-005GV, 0-5psi) and is referred to below as the pressure drop ΔP, which can vary in time. The listed output voltage for the OMEGA PX26-005GV pressure transducer is 50 mV at 5 psi . In order to maintain accuracy for readings at lower pressures, an instrumentation amplifier circuit is used to amplify the voltage output of the sensor to a range that is easily readable by available equipment. The circuit is constructed from three op-amps (Texas Instruments UA747), two of which serve as input buffers for the third, which is wired as a standard differential amplifier. This approach allows for accurate pressure readings from 690 Pa to 34.5 kPa in the current experiments (or as low as 200 Pa if needed). The output voltage of the circuit is calibrated by applying a known hydrostatic pressure to the pressure transducer. It is important to note that the voltage output is sensitive to changes in the power input to the sensor, so a consistent voltage supply should be used.

With the goal of measuring pressure fluctuations in mind, we note that there are several possible limitations on the resolution of the fluctuations (e.g. [10]). For our experiments, the response frequency of the pressure transducer is 1000 Hz and the sampling frequency of the data acquisition is 60 Hz. The frequency scales associated with flow through the channel range from 5 – 15 Hz, based on the range of mean flowrates. Therefore, as discussed further below, the sampling frequency of the pressure transducer is much higher than the measured frequency of the pressure fluctuations. Frequencies lower than 5 Hz reflect oscillations of the channel as one self-contained element within the microfluidic network and do not indicate well-resolved waveforms within the channel geometry itself.

We use Sylgard 184 to fabricate the PDMS microchannels. To study the effect of the elasticity of the microchannels on the pressure fluctuations, different Young's moduli E of PDMS are compared in the same microchannel system. The Young's modulus of PDMS is determined by the mixing ratio, the heating temperature and the heating time. [17–19] For PDMS fabrication, the mixing ratios of the base polymer to the curing agent are chosen as 15 to 1 and 5 to 1, and heating occurs at the curing temperature of 70°C for 10 h. The PDMS channel is connected to the syringes and pressure transducers by polytetrafluoroethylene (PTFE) tubing with inner diameter 0.6 mm, thereby forming a network of the pump, pressure transducer, and channel. The Young's modulus of PTFE is approximately two orders of magnitude larger than that of PDMS, and therefore the effect of the elasticity of the connecting tubing on the pressure fluctuations within the network is neglected.

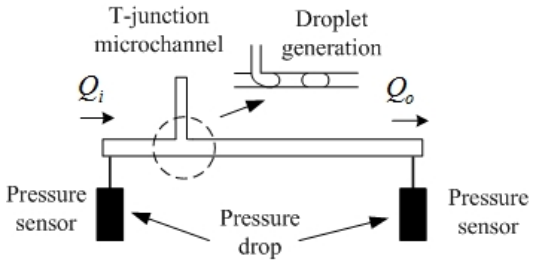

Fig. 1 Simplified model of the experimental system, where Q_i and Q_0 denote, respectively, the input and output flow rates. For the experiments on drop generation, we use the same device.

For the two-phase flow experiments reported in Section 5, water-in-oil droplets are generated in the T-junction microchannel, where the viscosity μ_w of the deionized water used is 1 cP, the viscosity μ_o of silicone oil is 5 cP, and the interfacial tension is $\gamma = 40$ mN/m. The values of all the experimental parameters are given in Table 1. The capillary number, $\mathrm{Ca} = \frac{\mu_o v}{\gamma}$, where v is a typical speed, characterizes two-phase for water drops in oil. For typical values of our experiments $\mathrm{Ca} \approx 0.1$.

3 Pressure fluctuations measurement

We define $\langle \Delta P \rangle$ as the mean pressure drop and $\widetilde{\Delta P}(t)$ as the pressure drop fluctuations. Then, the instantaneous pressure drop $\Delta P(t)$ is

$$\Delta P(t) = \langle \Delta P \rangle + \widetilde{\Delta P}(t) \tag{1}$$

For the same PDMS device, different diameters of syringes are tested. In a typical experiment, after a steady flow is established, which takes about 2 minutes, the gauge pressure at the inlet of the PDMS microchannel is measured, and gives the pressure drop $\Delta P(t)$. Fig. 2 shows time traces of the instantaneous pressure drop $\Delta P(t)$ normalized by the mean pressure drop $\langle \Delta P \rangle$ for a fixed mean flow rate of the syringe pump. It can be seen that both the amplitude and frequency of the pressure fluctuations vary with the syringe diameter. In particular, the pressure fluctuations are approximately time-periodic

Table 1 Parameters of the microchannel, syringe and fluid.

Explanation	Variables	Values
Channel width	w (um)	100
Channel height	h (um)	10
Channel length	l (mm)	100
Syringe diameters (1 ml)	D_1 (mm)	4.69
(2.5 ml)	D_2 (mm)	9.60
(5 ml)	D_3 (mm)	12.45
(10 ml)	D_4 (mm)	15.90
Viscosity of water	μ_w (cP)	1
Viscosity of silicone oil	μ_o (cP)	5
Interfacial tension	γ (mN/m)	40
Young's modulus of PTFE	E_0 (MPa)	$(6\pm2)\times10^2$
Young's modulus of PDMS	E_1 (MPa)	1.0 ± 0.1
Young's modulus of PDMS	E_2 (MPa)	2.0 ± 0.1
Pitch for syringe pump screw	s (mm)	1.056
Constant in equation (4)[8]	c	0.8 ± 0.2

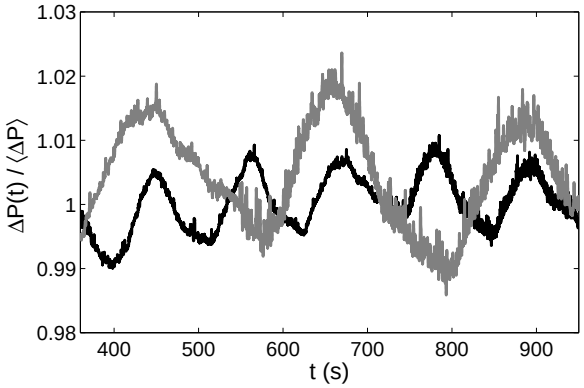

Fig. 2 Measured pressure fluctuations in a PDMS microchannel. Young's modulus of PDMS: E=1.0 ± 0.07 MPa, the mean inlet flow rate of syringe pump: $\langle Q_i\rangle$=0.02 ml/min, dark line D= 12.45 mm and light line D=15.90 mm.

and the smaller amplitude, higher frequency fluctuations occur for the smaller diameter syringe. Moreover, for the syringe of larger diameter, the amplitude of the pressure fluctuations reaches nearly 3% of the mean pressure drop $\langle\Delta P\rangle$. Also, we note that the absolute amplitude of the pressure fluctuations is about 1.0 kPa, and the frequency f of the pressure fluctuations is about 0.01 Hz.

The measured frequency f of pressure fluctuations is expected to follow the inherent mechanical frequency f_i of the screw-driven syringe pump[20], which varies with the syringe diameter D and mean inlet flow rate $\langle Q_i\rangle$ according to

$$f_i = \frac{4\langle Q_i\rangle}{\pi D^2 s}, \tag{2}$$

where s is the pitch of the screw in the syringe pump. Fig. 3 shows the measured frequency f of pressure fluctuations plotted against the mean inlet flow rate for four syringe diameters: the dotted lines show the prediction of the mechanical frequency f_i from equation (2), and the ratio f/f_i is shown in the inset of Fig. 3. For the inlet flow rates ranging from 0.03 - 0.09 ml/min, the deviation between f and f_i is smaller than 10%.

We next quantify the amplitude of the pressure fluctuations using the root-mean-square of the pressure drop fluctuations ΔP_{rms} normalized by the mean pressure drop $\langle\Delta P\rangle$, as shown in Fig. 4, which includes the results of different syringe diameters D, mean inlet flow rates $\langle Q_i\rangle$ and Young's moduli E. We note that the normalized amplitude $\Delta P_{rms}/\langle\Delta P\rangle$ of pressure fluctuations varies by two orders of magnitude over two decades in mechanical frequency f_i, and can be reduced by decreasing the Young's modulus E of the channel for the same mechanical frequency of the syringe pump.

4 Mathematical model

For a closed channel, continuity dictates that the difference between the inlet flow rate Q_i and the outlet flow rate Q_o is equal to the time rate change of the volume V of the channel itself, where the volume ($V = whl$) is equal to the product of the width, height, and length of the channel, respectively. As the typical flows are incompressible, the continuity of the flow rate can be expressed as

$$Q_i - Q_o = \frac{dV}{dt} \tag{3}$$

If $w \gg h$, the resistance of the channel is controlled mainly by h, so the change in the height of the channel induced by the pressure field needs to be considered. The actual height can then be expressed as $h_0 + \Delta h$, where h_0 is the undeformed channel height and Δh is the deformation of the channel. This deformation is a function of the maximum pressure[7], which is set by the pressure drop ΔP. Hence, the typical magnitude of channel deformation can be expressed as

$$\Delta h = c\frac{w\Delta P}{E} \tag{4}$$

where c is an order-one constant[8], which is determined by the stiffness of the microchannel. In our experiments, the thickness of the PDMS microchannel is 2 mm, so by linear interpolation of published results[8] based on the thickness of the channel wall, we estimate $c \approx 0.8\pm0.2$.

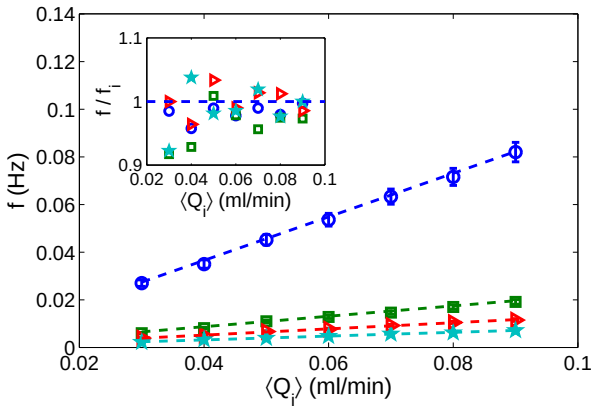

Fig. 3 Measured frequency of pressure fluctuations relative to the mechanical frequency of the syringe pump under different flow rates. Syringe diameters: ○ $D = 4.69$ mm; □ $D = 9.60$ mm; ▷ $D = 12.45$ mm;☆ $D = 15.90$ mm. The mechanical frequency predicted for each inlet flow rate is defined by the dotted lines − − −. The inset shows that the ratio of the measured (f) to the predicted (f_i) frequencies is nearly constant, independent of the mean inlet flow rate.

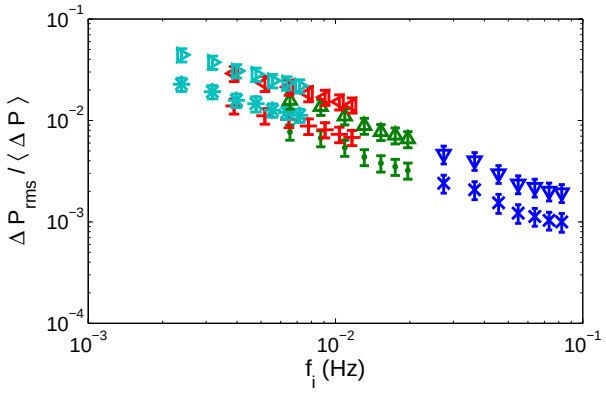

Fig. 4 A log-log plot of the mechanical frequency of the syringe pump and the normalized amplitude of pressure fluctuations. Young's modulus of PDMS: E=1.0 ± 0.07 MPa, experimental syringe diameters: × $D = 4.69$ mm; • $D = 9.60$ mm; + $D = 12.45$ mm;∗ $D = 15.90$ mm. Young's modulus of PDMS: E=2.0 ± 0.12 MPa, experimental syringe diameters: ▽ $D = 4.69$ mm; △ $D = 9.60$ mm; ◁ $D = 12.45$ mm; ▷ $D = 15.90$ mm.

The inlet flow rate is specified by the pump, and the outlet flow rate is assumed to be a linear function of the pressure drop between the inlet of the channel and the outlet. By using the model of Poiseuille flow and allowing for the deformation Δh of the channel height, the outlet flow rate can be described approximately by

$$Q_o = \frac{wh^3}{12\mu l}\left(1+\frac{\Delta h}{h}\right)^3 \Delta P \tag{5}$$

where μ is the fluid viscosity of the single-phase flow. By linearizing the outlet flow rate Q_o with respect to Δh, substituting equations (5) and (4) into (3), with volume $V = wl(h+\Delta h)$, we obtain

$$Q_i = \frac{cw^2 l}{E}\frac{d\Delta P}{dt} + \frac{wh^3}{12\mu l}\Delta P, \tag{6}$$

which was also obtained in the analysis of Leslie et al. [11]

Assuming the flow rate of the pump is a periodic function of time, we define $\langle Q_i \rangle$ as the mean flow rate of the pump and $\widetilde{Q}_i(t)$ as the flow-rate fluctuations. We take $\widetilde{Q}_i(t) = \sqrt{2}Q_{rms}\cos(2\pi f_i t)$, substitute into equation (6) and integrate, which yields the pressure drop

$$\Delta P(t) = \frac{wh^3}{12\mu l}\langle Q_i \rangle + \frac{\sqrt{2}Q_{rms}}{\sqrt{\left(\frac{wh^3}{12\mu l}\right)^2 + \left(\frac{2\pi c w^2 l}{E}\right)^2 f_i^2}}\cos(2\pi f_i t - \phi) \tag{7}$$

where $\phi = \arccos\left[1+\left(\frac{24\pi c\mu w l^2}{Eh^3}\right)^2 f_i^2\right]^{-\frac{1}{2}}$ is the phase delay of the pressure compared with the flow rate.

Subtracting the mean pressure drop from equation (7), taking the root-mean-square and rewriting in terms of the normalized amplitude $Q_{rms}/\langle Q_i \rangle$ of the flow-rate fluctuations, then the normalized amplitude of pressure fluctuations becomes

$$\frac{\Delta P_{rms}}{\langle \Delta P \rangle} = \frac{1}{\sqrt{1+St^2}}\frac{Q_{rms}}{\langle Q_i \rangle} \tag{8}$$

where

$$St = 24\pi c\left(\frac{wl^2}{h^3}\right)\left(\frac{\mu f_i}{E}\right) \tag{9}$$

The dimensionless parameter St represents a type of Strouhal number for the oscillations of the elastic channel system. This Strouhal number is a non-dimensional frequency that incorporates the mechanical frequency f_i of the pump, the frequency E/μ associated with the fluid-structure interaction, and the geometrical parameters of the microchannel. However, in order to test the model prediction of equation (8) for the overall behavior of pressure fluctuations, the normalized amplitude $Q_{rms}/\langle Q_i \rangle$ of flow-rate fluctuations needs to be estimated.

5 Estimating flow-rate fluctuations

One way to measure the flow-rate fluctuations, which has practical significance in many experiments, is by using a two-phase flow, forming droplets, and measuring the length of the droplets. For example, it is known that in a T-junction microchannel, the length of the droplets is correlated with the flow-rate ratio of the two immiscible fluids. Thus, we expect that at low capillary numbers (Ca ≪ 1), the length of the

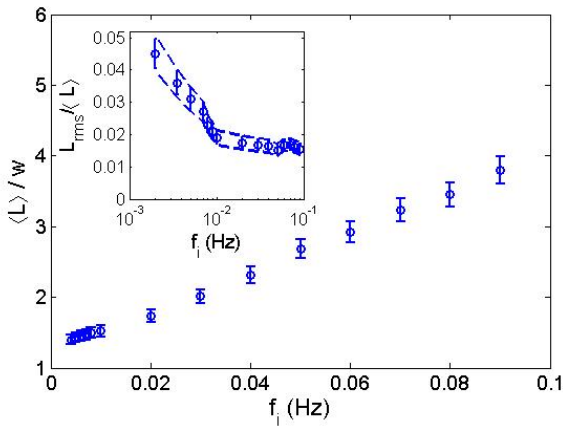

Fig. 5 Measured length of droplets under different mechanical frequencies f_i of the syringe pump. w is the width of the microchannel, $\langle L\rangle$ is the mean value of droplet length and $L_{rms}/\langle L\rangle$ is the normalized amplitude of droplet length fluctuations. The data can be fit with the linear equation $\langle L\rangle/w = c_1 Q_i/Q_0 + c_2$, where $Q_0 = 0.2$ ml/min is a constant and Q_i is changing and c_i are constants; from the data we estimate $c_1 = 1.5$ and $c_2 = 0.3$.The inset shows that the normalized amplitude of droplet length fluctuations varies with the mechanical frequency (different flow rates) of the syringe pump. The same syringe diameter was used in all of these experiments.

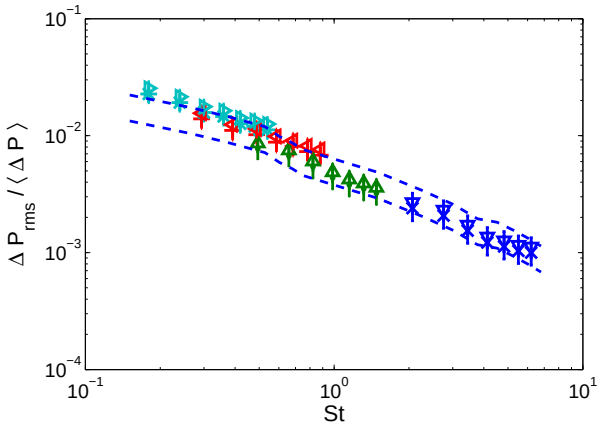

Fig. 6 A log-log plot of the non-dimensional Strouhal number and the amplitude of pressure fluctuations. Young's modulus of PDMS: E=1.0 ± 0.07 MPa,syringe diameters: × D = 4.69 mm; • D = 9.60 mm; + D = 12.45 mm;∗ D = 15.90 mm. Young's modulus of PDMS: E=2.0 ± 0.12 MPa, syringe diameters: ▽ D = 4.69 mm; △ D = 9.60 mm; ◁ D = 12.45 mm; ▷ D = 15.90 mm. The confidence interval of the model prediction is defined by the two dotted lines: – – –.

droplets is a linear function of the flow-rate ratio of the two immiscible fluids.[21] If there are periodic flow-rate fluctuations, the lengths of the droplets also vary in time.[20] In our experiments, the frequency of drop formation, and our sampling frequency, are much larger than the mechanical pump frequency f_i. Hence, we are able to detect fluctuations in drop length, which in turn provide estimates of (the more slowly changing) fluctuations in flow rate.

Using the same T-junction microchannel as above, we now report our results for droplet generation. Here, water is chosen as the dispersed phase and silicone oil is chosen as the continuous phase. The flow rate of the continuous phase is specified as 0.09 ml/min, so the capillary number Ca of droplet generation is about 0.2. The diameter of the syringe used for droplet generation is 12.45 mm (similar results were obtained for 9.60 mm and 15.90 mm diameter syringes). The flow rate of the syringe pump varies from 0.01 - 0.65 ml/min, and the mechanical frequency of the syringe pump varies from 0.002 - 0.09 Hz, which is comparable to the range studied for the measured pressure fluctuations above. Water-in-oil droplets are generated in the T-junction microchannel, with frequencies ranging from 50 - 100 Hz, which is much higher than the mechanical frequency f_i of the syringe pump. We use a high-speed camera to capture images of drops, with a frame rate 1000 fps (and typically 5-8 drops per frame). By using image-processing software in Matlab, the length of individual droplets is measured. Fig. 5 shows the results of droplet length as a function of the mechanical frequency f_i. Here, the mean length $\langle L\rangle$ of droplets is normalized by the channel width w, and the root-mean-square of droplet length fluctuations L_{rms} is normalized by the mean droplet length $\langle L\rangle$.

From Fig. 5, the mean length of droplets varies linearly with the flow rate of the syringe pump, as expected given that the droplet generation rate is much faster than the frequency of operation of the syringe pump. Also, the normalized amplitude $L_{rms}/\langle L\rangle$ of droplet length fluctuations varies with the flow rate of the syringe pump, as shown in the inset of Fig. 5. We observe that $L_{rms}/\langle L\rangle$ decreases as the flow rate increases, and becomes nearly constant at higher flow rates, with about a 10% deviation shown via the error bars. The fluctuations are higher at lower frequencies, as indicated previously by Kim et al.[9] As the syringe pump is driven by a stepper motor (1.8° for each step in this experiment), the mechanical oscillations significantly increase as the motor rotation speed decreases. Therefore, droplet generation becomes steadier as the mechanical frequency f_i increases, which helps to rationalize the measured $L_{rms}/\langle L\rangle$ (see inset to Fig. 5).

Based on the measurements $L_{rms}/\langle L\rangle$ of droplet length fluctuations, the normalized amplitude $Q_{rms}/\langle Q_i\rangle$ of flow-rate fluctuations can be estimated as a function of frequency. In particular, we can represent the data in Fig. 5 as $\langle L\rangle/w = c_1 Q_i/Q_0 + c_2$, where $Q_0 = 0.2$ ml/min is a constant and Q_i is changing and c_i are constants; from the data in Fig. 5 we esti-

mate $c_1 = 1.5$ and $c_2 = 0.3$. Then, based on our rapid sampling, we can conclude that $\frac{Q_{rms}}{\langle Q_i \rangle} = \frac{L_{rms}}{\langle L \rangle}$ (inset of Fig. 5).

Next, we use the estimation of $Q_{rms}/\langle Q_i \rangle$ to complete the model prediction of the pressure drop fluctuations, equation (8). Replotting the normalized amplitude $\Delta P_{rms}/\langle \Delta P \rangle$ from Fig. 4 using the non-dimensional Strouhal number defined in equation (9) allows a collapse of the experimental results for the two different Young's moduli of PDMS we used, as shown in Fig. 6. Based on the uncertainties in the estimate of $Q_{rms}/\langle Q_i \rangle$, the confidence interval of the model predictions is plotted with two dotted lines in Fig. 6, where we used equation (8) with the measured values of $Q_{rms}/\langle Q_i \rangle$. There are no fitting parameters here, as all parameters are known or measured, and the experimental results are mainly within the confidence interval of the model predictions. The slight under-prediction of the pressure fluctuations at lower Strouhal numbers may indicate a possible under-estimation of the flow-rate fluctuations at low frequencies, in the range where the syringe pump stepper motor becomes less reliable, as noted above, although the discrepancy is nearly within the limits of experimental error.

From the above analysis, in syringe-pump-driven microfluidic systems, the normalized amplitude of pressure fluctuations can be quantified based on the Strouhal number. For a specific flow-rate fluctuation of the syringe pump, by increasing the Strouhal number, the normalized amplitude of pressure fluctuations is reduced significantly, which improves the stability of the flow.

6 Conclusions

In syringe-pump-driven microfluidic systems, pressure fluctuations are observed in an elastic microchannel. The syringe pump is driven by an electrical stepper motor, from which mechanical oscillations are expected to generate flow-rate fluctuations and in turn leads to the pressure fluctuations in the channel flow. We confirmed that the frequency of pressure fluctuations is consistent with the mechanical frequency of the syringe pump.

Most importantly, we developed a mathematical model of the pressure fluctuations in an elastic microchannel. As the flow rate of the syringe pump increases, the amplitude of pressure fluctuations is affected mainly by the mechanical frequency of the pump. For a specific microfluidic device, the normalized amplitude of pressure fluctuations is reduced as the mechanical frequency of the syringe pump increases, but varies with the Young's modulus of the channel material, as captured by the Strouhal number dependence in equation (8). By increasing the Strouhal number, the amplitude of pressure fluctuations in an elastic microchannel is greatly reduced, which improves the stability of syringe-pump-driven microfluidic flows.

Acknowledgements

This work was supported by the National Natural Science Foundation of China (No: 51175101). The authors thank Dr. Saurabh Vjawahare and the Princeton University Microfluidic Laboratory for the fabrication of the microfluidic devices.

References

1 A. J. deMello, *Nature*, 2006, **442**, 394–402.
2 J. El-Ali, P. K. Sorger and K. F. Jensen, *Nature*, 2006, **442**, 403–411.
3 D. B. Weibel and G. M. Whitesides, *Curr. Opin. Chem. Biol.*, 2006, **12**, 584–591.
4 T. Thorsen, R. W. Roberts, F. H. Arnold and S. R. Quake, *Phys.Rev. Lett.*, 2001, **86**, 4163–4166.
5 S. Y. Teh, R. Lin, L. H. Hungb and A. P. Lee, *Lab on a Chip*, 2008, **8**, 198–220.
6 Z. Li, S. Y. Mak, A. Sauret and H. C. Shum, *Lab on a Chip*, 2014, **14**, 744–749.
7 T. Gervais, J. El-Ali, A. Gunther and K. F. Jensen, *Lab on a Chip*, 2006, **6**, 500–507.
8 B. S. Hardy, K. Uechi, J. Zhen and H. P. Kavehpour, *Lab on a Chip*, 2009, **9**, 935–938.
9 D. Kim, N. C. Chesler and D. J. Beebe, *Lab on a Chip*, 2006, **6**, 639–644.
10 P. Cheung, K. Toda-Peters and A. Q. Shen, *Biomicrofluidics*, 2012, **6**, 26501–26505.
11 D. C. Leslie, C. J. Easley, E. Seker, J. M. Karlinsey, M. Utz, M. R. Begley and J. P. Landers, *Nature Physics.*, 2009, **5**, 231–235.
12 K. W. Bong, S. C. Chapin, D. C. Pregibon, D. Baah, T. M. Floyd-Smith and P. S. Doyle, *Lab on a Chip*, 2011, **11**, 743–747.
13 Y. Wang, K. Sefiane, Z. G. Wang and S. Harmand, *Heat and Mass Transfer*, 2014, **70**, 353–362.
14 M. Heil and J. Boyle, *J. Fluid Mech.*, 2010, **652**, 405–426.
15 M. Heil and A. L. Hazel, *Annu. Rev. Fluid Mech.*, 2011, **43**, 141–162.
16 C. Bertram and J. Tscherry, *Journal of Fluids and Structures*, 2006, **22**, 1029–1045.
17 T. K. Kim, J. K. Kim and O. C. Jeong, *Microelectronic Engineering*, 2011, **88**, 1982–1985.
18 F. Schneider, J. Draheim, R. Kamberger and UlrikeWallrabe, *Sensors and Actuators A*, 2009, **151**, 95–99.
19 I. D. Johnston, D. K. McCluskey, C. K. L. Tan and M. C. Tracey, *J. Micromech. Microeng.*, 2014, **24**, 5017–5024.
20 P. M. Korczyk, O. Cybulski, S. Makulskaa and P. Garstecki, *Lab on a Chip*, 2011, **11**, 173–175.
21 P. Garstecki, M. J. Fuerstman, H. A. Stone and G. M. Whitesides, *Lab on a Chip*, 2006, **6**, 437–446.